

## Supplementary data

### **Nanoscale surface engineered magneto-mechano-triboelectric nanogenerator enabled by reliable pattern replication for self-powered IoT devices**

Srinivas Pattipaka,<sup>a†</sup> Tae Wan Park,<sup>a†</sup> Young Min Bae,<sup>a†</sup> Yujin Na,<sup>b</sup> Kyeongwoon Chung,<sup>c</sup> Kwi-Il Park,<sup>b</sup> Jungho Ryu,<sup>d</sup> Woon Ik Park,<sup>a\*</sup> and Geon-Tae Hwang<sup>a\*</sup>

<sup>a</sup>Department of Materials Science and Engineering, Pukyong National University, 45, Yongso-ro, Nam-Gu, Busan 48513, Republic of Korea.

<sup>b</sup>School of Materials Science and Engineering, Kyungpook National University, 80 Daehak-ro, Buk-gu, Daegu 41566, Republic of Korea.

<sup>c</sup>Department of Biofibers and Biomaterials Science, Kyungpook National University, Daegu, 41566, Republic of Korea.

<sup>d</sup>School of Materials Science and Engineering, Yeungnam University, Daehak-ro, Gyeongsang-si, Gyeongsangbuk-do 38541, Republic of Korea.

\*Corresponding authors

E-mail addresses: [gthwang@pknu.ac.kr](mailto:gthwang@pknu.ac.kr) (G. T. Hwang), [thane0428@pknu.ac.kr](mailto:thane0428@pknu.ac.kr) (W. I. Park)

<sup>†</sup>These authors contributed equally to this work.

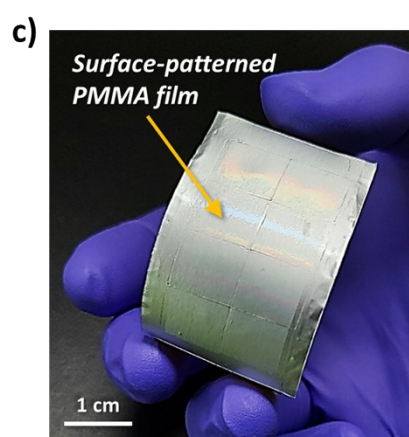
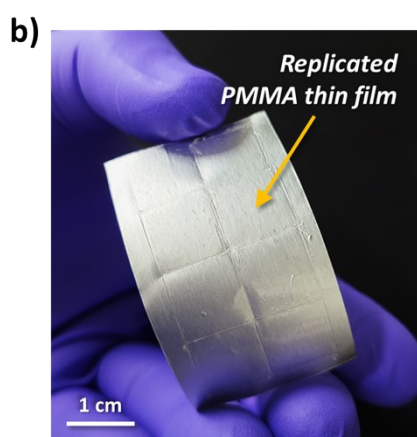
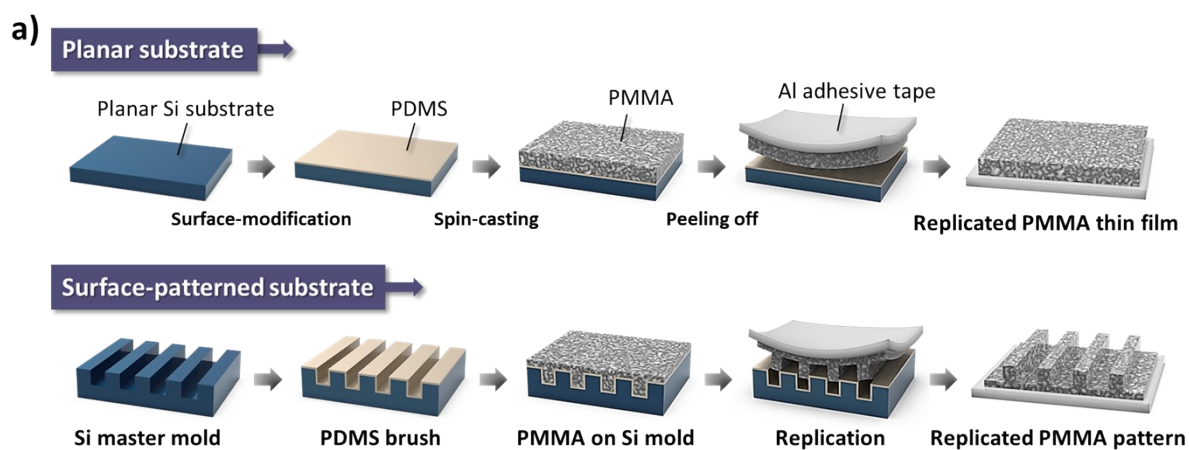


**Fig. S1.** (a) Sequential replication processes using a planar substrate and a surface-patterned Si master mold. Photographs of (b) PMMA film without pattern and (c) surface-patterned PMMA film.

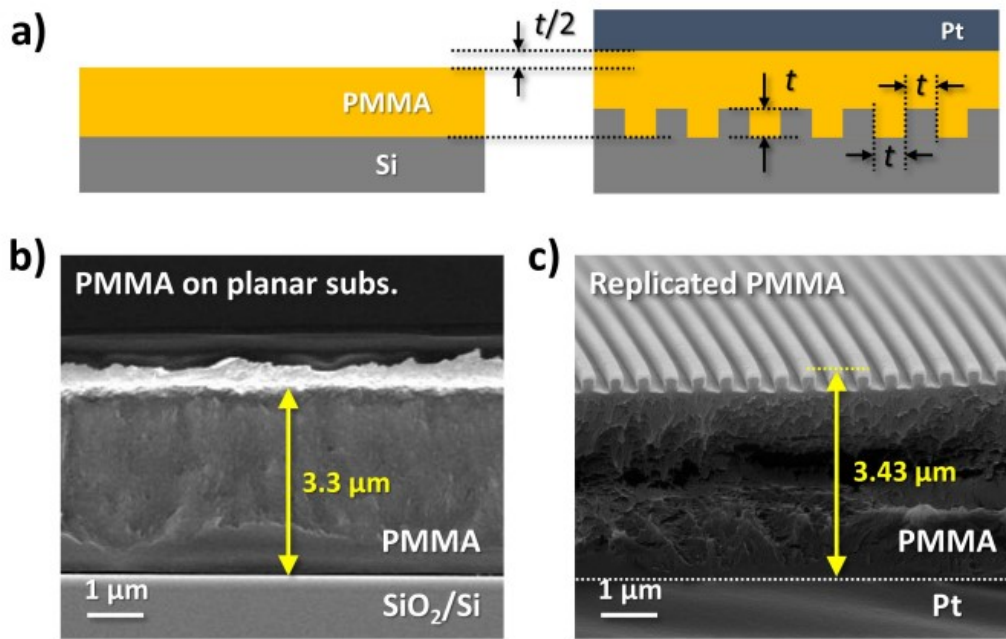


**Fig. S2.** (a) Schematic illustrations for the thickness of spin-casted PMMA 20 wt% solution on the planar and surface-patterned substrates. SEM images of (b) spin-casted PMMA thin film on planar  $\text{SiO}_2/\text{Si}$  substrate and (c) replicated PMMA film from the surface-patterned Si master mold (line width/line space/depth: 250 nm).

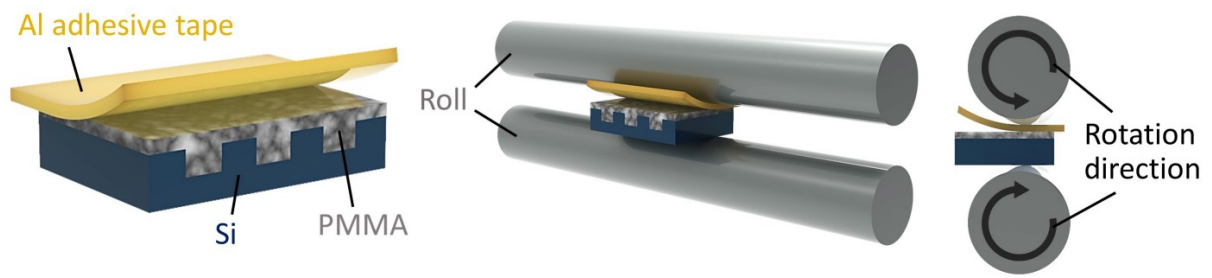


**Fig. S3.** Pattern replication of the triboelectric PMMA material by the rolling-press system, which can effectively provide a uniform contact pressure.

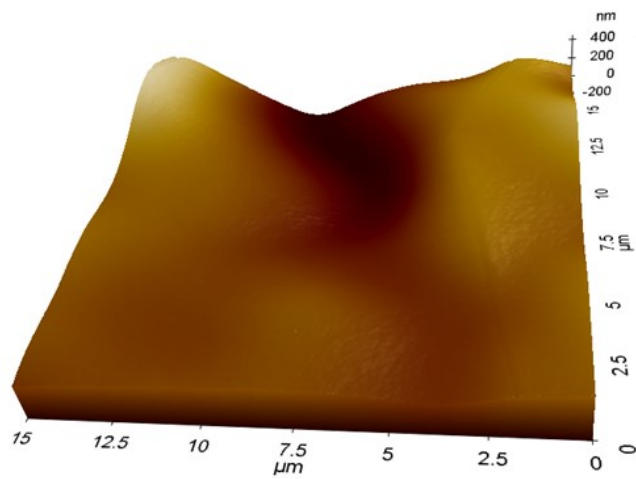


**Fig. S4.** The surface AFM image of pristine PMMA film.

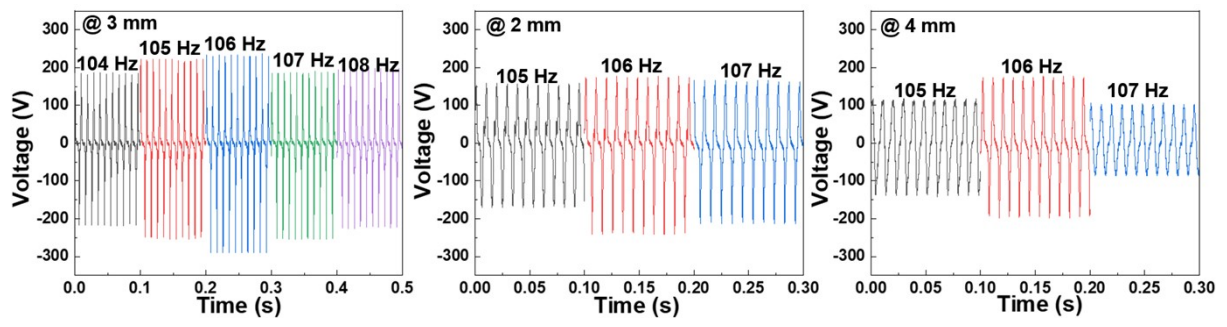


**Fig. S5.** Output voltage response of nano-patterned MMTNG measured at various frequencies of AC magnetic field and gap distances of triboelectric materials.

The contact electrification and electrostatic induction determine the amount of charge transferred and induced in the triboelectric layer<sup>14,15</sup>. When an alternating magnetic field is applied to the triboelectric layers doped with ferromagnetic materials, the charges become compelled to move in one direction, leading to improve output performance of the triboelectric nanogenerator<sup>15</sup>. In the case of non-ferromagnetic materials, they do not respond to the magnetic fields due to the absence of magnetic moments and domains. Therefore, induced magnetic force can't affect the charge distribution and transfer on the surface of triboelectric materials during the energy conversion process of MMTENG. Note that the alternating magnetic field was applied only to produce periodic up and down vibrations of the cantilever-structured MMTENG for contact triboelectrification and electrostatic induction. However, we measured the output voltage of the nano-patterned triboelectric nanogenerator device by utilizing a pushing machine without and with applied AC magnetic fields (500 Oe at 106 Hz) to verify this effect, as shown in Fig. S6. It is revealed that a stable output voltage without and with AC magnetic fields. Therefore, the alternating magnetic field can't affect the transfer of triboelectric charges during the energy conversion process of the MMTENG device.

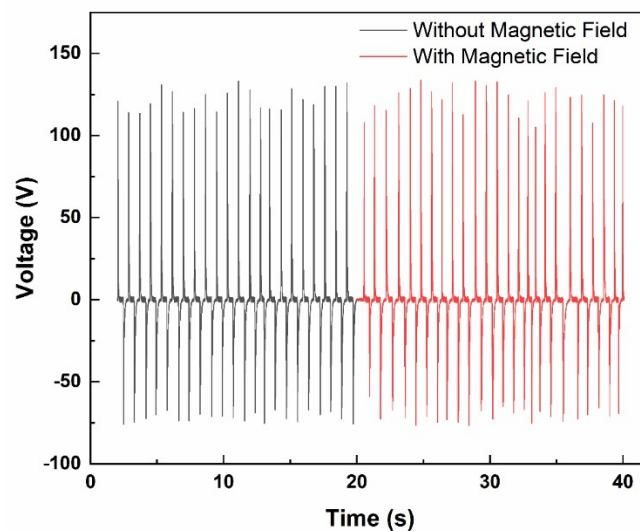


**Fig. S6.** Output voltage response of nano-patterned triboelectric nanogenerator without and with applied AC magnetic fields (500 Oe at 106 Hz) by contact and separation motions on a pushing machine.

**Table S1.** Comparison of the output performance between MMTENG and conventional TENGs.

Energy Source	Structure	Open-circuit Voltage	Short-circuit current	Reference
AC magnetic field	Cantilever	300 V	177 $\mu$ A	This work
Wind	Free-standing Wing	100 V	80 $\mu$ A	Ya et al <sup>3</sup>
Water wave	Buoy	280 V	120 $\mu$ A	Xi et al <sup>4</sup>
Mechanical force	contact-sliding-separation structure	1238 V	48.7 $\mu$ A	Yang et al <sup>5</sup>
Mechanical vibration	harmonic-resonator	288 V	77 $\mu$ A	Jun et al <sup>6</sup>

#### References:

- 1 Z. L. Wang, *Faraday Discuss.*, 2014, **176**, 447–458.
- 2 Y. Li, G. Li, P. Zhang, H. Zhang, C. Ren, X. Shi, H. Cai, Y. Zhang, Y. Wang, Z. Guo, H. Li, G. Ding, H. Cai, Z. Yang, C. Zhang and Z. L. Wang, *Adv Energy Mater.*, , DOI:10.1002/aenm.202003921.
- 3 Y. Yang, G. Zhu, H. Zhang, J. Chen, X. Zhong, Z.-H. Lin, Y. Su, P. Bai, X. Wen and Z. L. Wang, *ACS Nano*, 2013, **7**, 9461–9468.
- 4 X. Liang, T. Jiang, G. Liu, Y. Feng, C. Zhang and Z. L. Wang, *Energy Environ Sci*, 2020, **13**, 277–285.
- 5 Y. Yu, Q. Gao, X. Zhang, D. Zhao, X. Xia, J. Wang, H. Li, Z. L. Wang and T. Cheng, *Energy Environ Sci*, 2023, **16**, 3932–3941.
- 6 J. Chen, G. Zhu, W. Yang, Q. Jing, P. Bai, Y. Yang, T. Hou and Z. L. Wang, *Advanced Materials*, 2013, **25**, 6094–6099.